

# Truncated Configuration Interaction expansions as solvers for correlated quantum impurity models and dynamical mean field theory

Dominika Zgid,<sup>1</sup> Emanuel Gull,<sup>2</sup> and Garnet Chan<sup>1</sup>

<sup>1</sup>*Department of Chemistry and Chemical Biology, Cornell University, Ithaca, New York, USA*

<sup>2</sup>*Max Planck Institut für Physik komplexer Systeme, Dresden, Germany*

The development of polynomial cost solvers for correlated quantum impurity models, with controllable errors, is a central challenge in quantum many-body physics, where these models find applications ranging from nano-science to the dynamical mean-field theory (DMFT). Here we describe how configuration interaction (CI) approximations to exact diagonalization (ED) may be used as solvers in DMFT. CI approximations retain the main advantages of ED, such as the ability to treat general interactions and off-diagonal hybridizations and to obtain real spectral information, but are of polynomial cost. Furthermore, their errors can be controlled by monitoring the convergence of physical quantities as a function of the CI hierarchy. Using benchmark DMFT applications, such as single-site DMFT of the 1D Hubbard model and  $2 \times 2$  cluster DMFT of the 2D Hubbard model, we show that CI approximations allow us to obtain near-exact ED results for a tiny fraction of the cost. This is true over the entire range of interaction strengths including “difficult” regimes, such as in the pseudogap phase of the 2D Hubbard model. We use the ability of CI approximations to treat large numbers of orbitals to demonstrate convergence of the bath representation in the  $2 \times 2$  cluster DMFT using a 24 bath orbital representation. CI approximations thus form a promising route to extend ED to problems that are currently difficult to study using other solvers such as continuous-time quantum Monte Carlo, including impurity models with large numbers of orbitals and general interactions.

PACS numbers: 71.10.Fd, 71.30.+h, 71.20.-b, 71.15.-m

## I. INTRODUCTION

Quantum impurity models describe a finite set of interacting “impurity” orbitals coupled to a large number of non-interacting “bath” or “lead” states. They were originally designed to describe the effect of magnetic impurities embedded in a non-magnetic host material<sup>1</sup>, but have since found a wide variety of applications ranging from nanoscience,<sup>2</sup> where they are used to describe quantum dots and molecular conductors, to surface science<sup>3</sup>, for the description of molecule adsorption on a substrate, to research in quantum field theories.<sup>4,5</sup> In recent years, they have gained an increasingly important role in condensed matter and materials science, where they appear as auxiliary models in the simulation of correlated lattice models within the so-called dynamical mean field theory (DMFT)<sup>6–8</sup> approximation and its extensions.<sup>9,10</sup>

A general quantum impurity model is described by the Hamiltonian

$$H = H_{\text{loc}} + H_{\text{bath}} + H_{\text{hyb}}, \quad (1)$$

$$H_{\text{loc}} = \sum_{pq} t_{pq} d_p^\dagger d_q + \sum_{pqrs} I_{pqrs} d_p^\dagger d_q^\dagger d_r d_s, \quad (2)$$

$$H_{\text{bath}} = \sum_{ki} \varepsilon_{ki} c_{ki}^\dagger c_{ki}, \quad (3)$$

$$H_{\text{hyb}} = \sum_{kip} V_{kip} c_{ki}^\dagger d_p + \text{h.c.} \quad (4)$$

$H_{\text{loc}}$  describes the “impurity” itself,  $H_{\text{bath}}$  a set of non-interacting “bath” or “lead” sites, and the impurity-bath coupling or “hybridization” is contained in  $H_{\text{hyb}}$ . The

operators  $d^{(\dagger)}$  and  $c^{(\dagger)}$  create and annihilate impurity and lead electrons,  $t$  and  $I$  describe the impurity hopping and interaction terms,  $\varepsilon$  a bath dispersion and  $V$  the impurity-bath hybridization strength.

The finite number of impurity interactions makes quantum impurity models numerically tractable. The development of accurate and reliable numerical solvers for correlated quantum impurity models is therefore one of the central challenges of computational many-body physics. Many different approaches have been proposed. Among those that can be made exact with sufficient computational effort, at least for some classes of models, are: quantum Monte Carlo methods, such as the continuous-time quantum Monte Carlo (CT-QMC);<sup>11</sup> renormalization group (RG) methods, including numerical<sup>12,13</sup> and density matrix RG<sup>14,15</sup>; and exact diagonalization (ED)<sup>16</sup>.

All these techniques have different strengths and weaknesses. For example, CT-QMC is formulated in imaginary time and real-frequency data at high frequencies, obtained with analytic continuation, is notoriously unreliable, while NRG has limited resolution in spectral quantities far from the Fermi surface and cannot be reliably extended beyond two impurity orbitals. ED does not suffer from the above two difficulties, but introduces a finite size error associated with a discrete bath representation. For some special Hamiltonians, such as those with density-density interactions and diagonal hybridizations, CT-QMC has no sign problem, and thus affords a polynomial time solution of the impurity problem. However, for general Hamiltonians, all the above techniques including CT-QMC exhibit an exponential scaling with

the number of impurity orbitals and, in the case of ED, with the number of bath orbitals. Consequently, there is an urgent need to develop controlled approximate solvers for general impurity models, where the exponential scaling is ameliorated or eliminated.

The dynamical mean-field theory and its cluster variants provide an ideal test bed for numerical quantum impurity solvers. DMFT is now established as a powerful theoretical framework for describing interacting quantum solids, both in the context of single-site multi-orbital and single-orbital cluster model Hamiltonians, as well as with realistic interactions within the DFT+DMFT<sup>9,17</sup> framework. In DMFT the bulk quantum problem is mapped onto a self-consistent quantum impurity model. Depending on the lattice model parameters, regions of weak, intermediate, and large correlation strengths can be accessed, and the wealth of previously computed data and the well-understood physics makes reliable comparisons possible.

Our present work presents controlled polynomial cost approximations to ED, using the idea of configuration interaction (CI)<sup>18</sup> that has long been studied in quantum chemistry. Recall that, at zero temperature, the Green's function is

$$ig_{ij}(\omega) = \langle \Psi | a_i^\dagger (\omega - H + E - i\eta)^{-1} a_j | \Psi \rangle + \langle \Psi | a_j (\omega + H - E + i\eta)^{-1} a_i^\dagger | \Psi \rangle \quad (5)$$

where  $E$  and  $\Psi$  are the ground-state energy and wavefunction of  $H$ . In ED, the true ground state wavefunction  $\Psi$  is expanded in the complete space of Slater determinants, and the size of the complete space, which scales exponentially as a function of the number of impurity and bath orbitals, is the primary limitation of the calculation. Even using state-of-the-art ED (Lanczos) codes, no more than 16 electrons in 16 orbitals (32 spin-orbitals) can be treated. CI approximates ED by solving for  $\Psi$  within a *restricted* variational space of Slater determinants. This variational space is constructed by including determinants based on their excitation level relative to a single, or multiple, physically motivated reference determinants. The various CI methods form a convergent hierarchy of approximations, where the variational space is systematically increased, and thus their error, relative to the theoretical ED limit, can be controlled by monitoring the convergence of the hierarchy. Furthermore, because CI methods exhibit a polynomial scaling with respect to the number of impurity and bath orbitals, they have the potential to treat much larger systems than ED. Indeed, in quantum chemistry, CI calculations with a thousand orbitals are routine.

The central question to answer in the context of correlated quantum impurity models is whether or not CI approximations form a sufficiently rapidly convergent hierarchy for the physical quantities of primary interest. If so, the ability to treat large numbers of orbitals and off-diagonal hybridizations, while retaining the strengths of ED, can be expected to be of great utility in revealing the

physics of complex quantum impurity models. In Ref. 19 we demonstrated that a very approximate CI solver could reproduce exact diagonalization results in a simple quantum impurity problem arising from the DMFT approximation to the cubic hydrogen solid. However, in that work our focus was not on the quality of the solver, but rather on chemical aspects of DMFT, such as the use of realistic Hamiltonians which do not suffer from double-counting. In the current work, we return to a systematic study of the CI approximations themselves. Since our target is to assess the quality of our approximations, we concentrate here on well-studied DMFT benchmark problems whose physics is understood, including single-site DMFT of the 1D Hubbard model and  $2 \times 2$  cluster DMFT of the 2D Hubbard model. The double-counting issue does not arise in these systems. As we will demonstrate, in these systems the CI approximations allow us to reproduce the ED calculations at a small fraction of the cost. Furthermore, because we can treat a larger number of orbitals than with ED, we will demonstrate that we can converge these models with respect to their bath representation. In the cases of the  $2 \times 2$  cluster DMFT approximation to the Hubbard model this has previously not been possible with ED (Lanczos).

The structure of this paper is as follows. In section II we first describe the theory behind CI approximations, including a detailed description of the excitation space, single- and multi-reference CI approximations, complete active spaces, and natural orbitals. In section III, we briefly describe some technical details of the implementation. In section IV we describe our application of CI solvers in model DMFT problems described above, using ED as a comparison where possible, and we demonstrate further the ability of CI to converge systems with large numbers of bath orbitals. Finally, we describe perspectives and conclusions in section V.

## II. CONFIGURATION INTERACTION APPROXIMATIONS

Configuration interaction (CI) wave functions  $|\Psi_{\text{CI}}\rangle$  are a set of systematic approximations to the ED wave function  $\Psi_{\text{ED}}$ . Using CI wave functions, the ground state of the impurity model is determined in a truncated subset of the complete set of Slater determinants. Once a ground state wave function is obtained, the impurity Green's function and self-energy, the central quantities in DMFT, are evaluated through Eq. (5). CI truncations rely on an *a priori* ranking of the importance of the determinants, in terms of excitation character relative to a single starting determinant (single-reference CI), or multiple starting determinants (multi-reference CI). This ranking is motivated by ordinary and degenerate perturbation theory, although CI approximations are not perturbative approximations *per se*. Note that the accuracy of CI truncations of the determinant space depends on the choice of orbital basis, and this is also an important

consideration in a CI calculation.

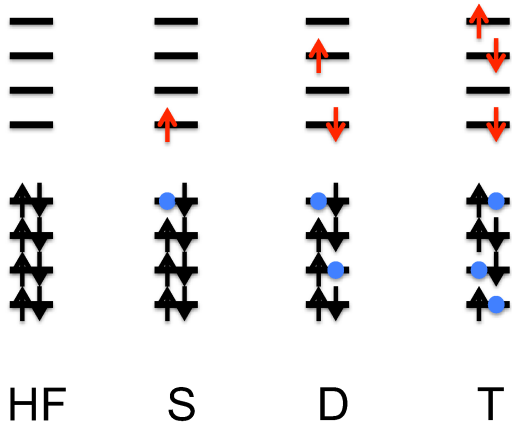


FIG. 1. Schematic of determinants included in configuration interaction approximations. HF denotes the Hartree-Fock determinant with a set of doubly occupied orbitals. S denotes a singles excitation, where one particle (arrow, red online) is excited out of a doubly occupied orbital (leaving a hole, dot, blue online). D and T denote doubly and triply excited configurations with respect to the Hartree Fock reference state.

We first motivate single-reference CI approximations using the Anderson model in the limit of small  $U$ . Here,  $\Psi$  is close to the Hartree-Fock (HF) determinant  $\Phi$ . Consequently, we take  $\Phi$  to be the (single) reference determinant in the CI. We next change from the site basis ( $d, d^\dagger, c, c^\dagger$ ) to the basis of HF orbitals ( $a, a^\dagger$ ), which are a mixture of impurity and bath orbitals. The determinants in the HF basis can be labeled in terms of excitation or particle-hole character relative to  $\Phi$ . For example, a singly-excited determinant  $\Phi_i^a = a_a^\dagger a_i(\Phi)$  has one particle and one hole relative to the HF determinant; the doubly-excited determinant  $\Phi_{ij}^{ab} = a_a^\dagger a_b^\dagger a_i a_j(\Phi)$  has two particles and holes, and so forth. To construct a CI approximation, we truncate the complete determinant space based on the maximum excitation character of determinants in the expansion of  $\Psi$ . For example, in a CI singles and doubles (CISD) approximation, we approximate  $\Psi$  with an expansion with at most doubly excited determinants (see Fig. 1),

$$|\Psi\rangle \approx c_0|\Phi\rangle + \sum_{i,a} c_i^a |\Phi_i^a\rangle + \sum_{ij,ab} c_{ij}^{ab} |\Phi_{ij}^{ab}\rangle. \quad (6)$$

More accurate CI approximations, with up to triple (CISDT), quadruple (CISDTQ) and higher excitations can be formulated in a similar way, and these systematically approach the full ED solution. However, for small  $U$ , we can expect CISD to already be a good approximation, because it contains all classes of determinants that couple with  $\Phi$  through first-order perturbation theory in  $U$ . Similarly, CISDTQ contains all classes of determinants that couple through second-order, and so on.

The above CI approximations (CISD, CISDT, etc.) are termed single-reference because the truncation of the determinant space is based on excitations relative to a single reference determinant  $\Phi$ . We expect this hierarchy of truncations to be rapidly convergent for small  $U$ , but for large  $U$  multiple determinants can become degenerate with  $\Phi$  on the scale of  $U$  and contribute with similar weights to  $\Psi$ . For example, in the single site Anderson model at large  $U$ ,  $\Psi$  is qualitatively given by a superposition of two determinants describing a ‘‘Kondo’’ singlet coupling of electrons of opposite spin on the impurity orbital and in the bath. In such cases, it is more reasonable to rank determinants with respect to a set of near-degenerate determinants. This is the basis of multi-reference CI approximations. Denoting the near-degenerate determinants as  $\Phi(I)$  (where  $I$  ranges over the degenerate set), then for each  $\Phi(I)$ , we can define singly, doubly, and higher excited determinants,  $\Phi_i^a(I) = a_a^\dagger a_i(\Phi(I))$ ,  $\Phi_{ij}^{ab}(I) = a_a^\dagger a_b^\dagger a_i a_j(\Phi(I))$ , and so on. In the multi-reference CI singles doubles approximation,  $\Psi$  is expanded in

$$|\Psi\rangle \approx \sum_I c_0(I) |\Phi(I)\rangle + \sum_I \sum_{i,a} c_i^a(I) |\Phi_i^a(I)\rangle \quad (7)$$

$$+ \sum_I \sum_{ij,ab} c_{ij}^{ab}(I) |\Phi_{ij}^{ab}(I)\rangle.$$

Multi-reference approximations including triples and higher excitations can be defined analogously.

One drawback of multi-reference CI calculations is that they are more difficult to set up and describe compactly, because of the need to identify the near-degenerate set of determinants  $\Phi(I)$ . A much simpler task is to specify only a set of near-degenerate orbitals, and to assume that all determinants obtained by considering different occupancies of the near-degenerate orbitals (with the remaining orbitals held empty or doubly occupied) constitute a near-degenerate set of references. This is the basis of the complete active space (CAS) specification of the references  $\Phi(I)$ . A  $\text{CAS}(n, m)$  set of references is obtained by identifying  $m$  near-degenerate orbitals, and constructing the determinants consisting of all distributions of  $n$  particles across the  $m$  orbitals. Once the CAS space is constructed, we can define a CASCI as above. For example, the CASCI approximation consists of expanding  $\Psi$  using a space of singles and doubles excitations out of the  $\text{CAS}(n, m)$  space as in Eq. (8) (see Fig. 2), and higher analogues are similarly defined. In this work, we will exclusively use CAS spaces when defining our multi-reference CI calculations.

### A. Improved orbitals

It is clear that the accuracy of a CI approximation is dependent on the orbitals used to specify the determinants. For small  $U$ , the HF orbital basis performs well. However, this is not always the best choice when  $U$  is

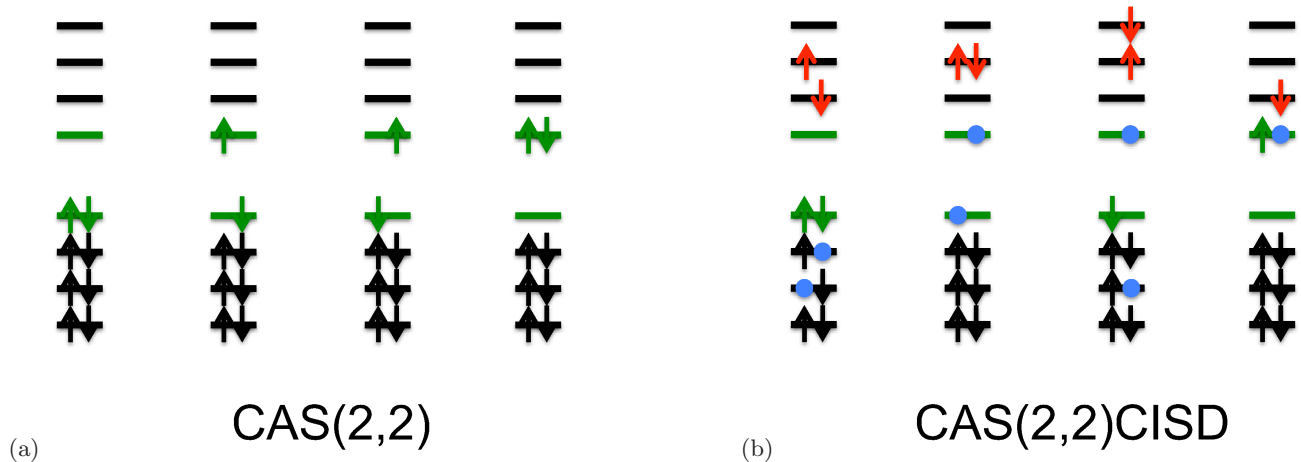


FIG. 2. (a): determinants in a CAS(2,2) complete active space. The light (green online) lines are the 2 “active” orbitals; the rest are denoted “inactive”. The four configurations correspond to the four ways of distributing 2 electrons across the 2 active orbitals. (b): examples of four of the determinants contained in a CAS(2,2)CISD approximation. Excitations may be from doubly occupied, non-active orbitals (first determinant), from active orbitals (second, fourth determinants), and from a mixture of active and inactive orbitals (third determinant).

large. The orbital basis which leads to the most rapid convergence of a complete CI expansion, as measured by one-particle density matrix norm, is called the *natural orbital* basis. Natural orbitals are eigenfunctions of the one-particle density matrix  $D_{ij} = \langle \Psi | a_i^\dagger a_j | \Psi \rangle$ , where  $\Psi$  is the exact or CI wavefunction; the corresponding eigenvalues are the natural occupancies. The natural orbital basis is a commonly used basis for CI calculations. Of course, the natural orbitals themselves are defined using  $\Psi$  which is not known until the CI calculation is performed. Consequently, a natural orbital based CI calculation is usually carried out in two steps.<sup>20</sup> First, a CI calculation in the Hartree-Fock basis is performed to obtain the density matrix. This is then diagonalized to obtain the natural orbitals, and the CI calculation is repeated in this basis. In principle, this procedure can be iterated, although we have not done so in the calculations in this work.

These procedures are standard in modern quantum chemistry and are commonly used to treat finite molecular systems. Detailed descriptions can be found in Refs. 18 and 21.

### III. IMPLEMENTATION

We have implemented the CI based approximations described above, as well as ED, within the context of single-site and cluster-based DMFT solvers. Our code uses a modified version of the efficient string-based CI algorithm in the DALTON quantum chemistry package.<sup>22</sup> The solution of the CI and ED eigenvalue problems is carried out using iterative Davidson diagonalization,<sup>23</sup> while the determination of the Green’s function in Eq. (5) is carried out using the Lanczos algorithm.<sup>24</sup> For the hybridiza-

tion and bath fitting necessary in the DMFT context, we have employed the procedures described in Ref. 19. The DMFT self-consistency was carried out until convergence in the self-energy was reached with a tolerance of less than 0.5%. All calculations were performed at  $T = 0$ , and all energies are in units of  $t = 1$ . The  $\beta$  used for fitting the dynamical mean field parameters were  $20/t$  (single site DMFT) and  $12.5/t$  (plaquette).

### IV. RESULTS

We now assess the performance of CI approximations as quantum impurity solvers using established benchmark problems. To recapitulate, the two central questions are: how rapidly do the CI approximations converge to ED, for example, as a function of excitation level or orbital basis, and, do CI approximations allow us to accurately treat a larger number of orbitals than ED? We found the impurity models occurring in the dynamical mean field context to be more difficult to solve than simple impurity sites coupled to an analytically constructed density of states, and we therefore focus our presentation on impurity models obtained within this context. We first study an impurity model without self-consistency imposed. We then examine two DMFT models. The first is the single site DMFT approximation to the 1D Hubbard model. Here, ED calculations can be converged with respect to the number of bath orbitals, which allows us to compare ED and CI approximations in the limit of a converged bath representation. Our second model is a  $2 \times 2$  plaquette (4-site) cellular dynamical mean field<sup>10,25</sup> calculation for the 2D Hubbard model. Such 4-site cluster models have been extensively studied with ED<sup>25–30</sup> as well as with CT-QMC,<sup>31–33</sup> and provide a standard

calibration point. We begin by comparing ED and CI approximations using an ED parametrization with 8 bath orbitals. Next, we demonstrate the ability of CI methods to treat large numbers of orbitals by converging the 4-site cluster model with respect to the number of bath orbitals in the parametrization. Our largest calculation involves 28 orbitals, significantly larger than can be treated with ED. In the appendix we present a three-orbital single site DMFT calculation of a model relevant for the physics of the  $t_{2g}$  bands in transition metal oxides. This model uses a Slater-Kanamori form of the impurity interaction.<sup>34,35</sup> We show that CI approximations can be used with a general impurity Hamiltonian with non-density-density interactions and demonstrate convergence of the bath representation with up to 24 orbitals.

### A. Anderson impurity model

As a test case for a quantum impurity model we present in Tab. I the parametrization for typical hybridization strengths and energy level parameters as they arise in the DMFT context, for  $U/t = 4$  at half filling. The Hamiltonian of this impurity model is

$$H = U \left( n_{\uparrow} n_{\downarrow} - \frac{n_{\uparrow} + n_{\downarrow}}{2} \right) + \sum_{i\sigma} \varepsilon_i c_{i\sigma}^{\dagger} c_{i\sigma} \quad (8)$$

$$+ \sum_{i\sigma} V_i c_{i\sigma}^{\dagger} d_{\sigma} + \text{h.c.}$$

The impurity model has one impurity site and eleven bath sites. In the particle-hole symmetric case, the choice of the active orbitals is motivated by the energetic degeneracy of the eigenvalues present already in the non-interacting Hamiltonian. The active orbitals for the CAS calculation are the orbitals 6 and 7 of the natural orbitals displayed (as obtained in ED) in Tab. II, which are singly occupied. We first remark on the sizes of the CI determinant spaces and the corresponding run-times which are given in Table III. We see that all the CI approximations involve only a small fraction of the full ED determinant space and take a much shorter amount of time to run. All of these calculations are doable within minutes on a desktop PC.

Fig. 3 shows results for the spectral function (upper panel) and the imaginary part of the self energy (lower panel) for the methods of Tab. III. All methods recover both the high- and the low-energy part of the self-energy to high accuracy. Differences in the spectral function are visible for  $\omega > 2$ , where higher excitations that are not contained within the approximations become important. Note that we intentionally use only a small imaginary broadening so as to preserve as much structure as possible and emphasize the difference between different approximations; This is why the spectral functions do not appear smooth.

Fig. 3 shows that for simple Anderson impurity models the truncated CI expansions are extremely robust, and

i	$\epsilon_i$	$V_i$
1	0.558819356316	0.553263286885
2	-0.558819356316	0.553263286885
3	4.45759206721	0.541358378777
4	-4.45759206721	0.541358378777
5	-1.47891491526	0.488524003875
6	1.47891491526	0.488524003875
7	-0.185401954358	0.383193040171
8	0.185401954358	0.383193040171
9	0.0317683411165	0.23348635632
10	-0.0317683411165	0.23348635632
11	0.0	1.e-5

TABLE I. Bath parametrization for a typical impurity problem with 12 sites (1 impurity site and 11 bath sites) obtained from converging ED, for which the spectral function and impurity self energy are reproduced in Fig. 3.

orbital number	1-4	5	6	7	8	9-12
$U/t = 4$	2.00	1.895	1.020	0.980	0.105	0.000
$U/t = 6$	2.00	1.738	1.009	0.991	0.262	0.000
$U/t = 8$	2.00	1.502	1.001	0.998	0.498	0.000
$U/t = 20$	2.00	2.000	1.000	1.000	0.000	0.000

TABLE II. Orbital occupancies in the natural orbital basis, for the impurity model of Tab. I. The choice of the active space is motivated by the partially occupied natural orbitals.

even low excitation levels can recover the proper self-energy. In the dynamical mean field context, an additional complication arises: the self-consistency condition and the bath fitting procedure lead to an amplification of differences that make the final result more sensitive to differences in the impurity self energy.

method	space size	$t_{GS}/t_{ED_{GS}}$	$t_{GF}/t_{ED_{GF}}$
CISD	1819	0.0026263	0.019265
CISDT	18819	0.012848	0.057334
CAS(2,2)CISD	6044	0.012242	0.035215
CAS(2,2)CISDT	49644	0.12739	0.13240
ED	853776	1	1

TABLE III. Size of determinant space for 12 electrons and 12 orbitals, and run-times in the solution of  $\Psi$ , using various CI approximations and ED.  $t_{GS}/t_{ED_{GS}}$  ( $t_{GF}/t_{ED_{GF}}$ ): runtime of ground state (Green's function) calculation with respect to ED ground state (Green's function) calculation.

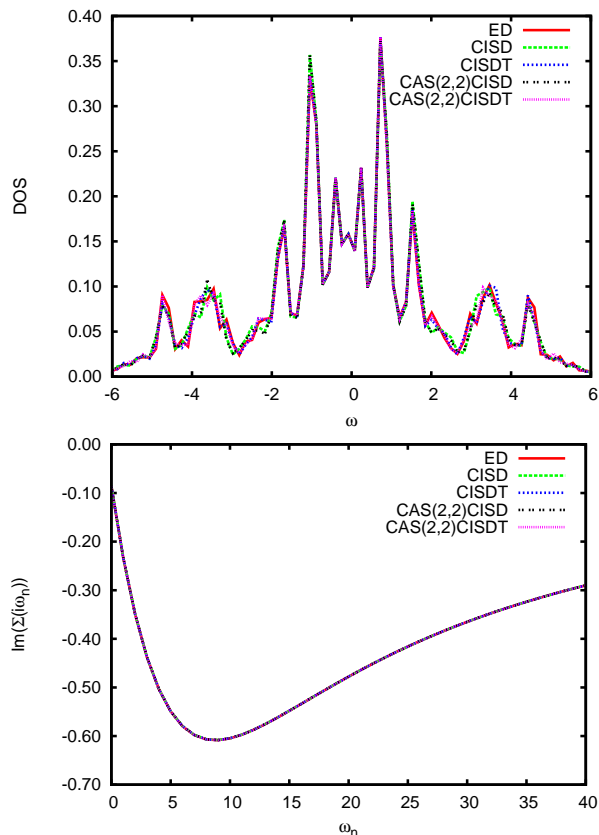


FIG. 3. Spectral function  $-\frac{1}{\pi}\text{Im}G(\omega)$  (upper panel) and the imaginary part of the self-energy  $\text{Im}\Sigma(i\omega_n)$  (lower panel) for an impurity model using the bath parametrization in Tab. I. Solid lines (red online): ED. Light dashed line (green online): CISD. Dark dashed line (blue online): CISDT. Double dotted line (black online): CAS(2,2)CISD. Dotted line (magenta online): CAS(2,2)CISDT.

## B. Single site DMFT for the 1D Hubbard model

### 1. particle-hole symmetric case

We carried out single site DMFT calculations for the 1D Hubbard model using an 11 orbital bath parametrization (12 orbitals in total). We used CISD, CISDT, CAS(2,2)CISD, CAS(2,2)CISDT approximations as well as ED to obtain the spectral functions and impurity self-energies for  $U/t = 4, 6, 8, 20$ . All calculations are performed in the natural orbital basis, as described in Sec. II A.

The spectral functions at half-filling are shown in Fig. 4. We observe good qualitative agreement of all CI methods with ED for all values of  $U/t$ . If we include triple excitations (CISDT or CAS(2,2)CISDT) the CI spectral functions become indistinguishable to the eye from ED. In the case of CISDT, this is achieved using only about 2% of the complete determinant space of ED. Perhaps surprisingly, multi-reference CI approximations are not necessary to obtain good agreement even

for large  $U/t$  where  $\Psi$  contains large weights from determinants other than the Hartree-Fock determinant. This reflects the simplicity of the 1D Hubbard model: the two main determinantal contributions to  $\Psi$  at large  $U$  differ in the occupancies of only two electrons, which can be adequately described using doubles excitations. It also reflects the non-perturbative nature of CI: so long as the determinants of interest are within the CI space, they can assume arbitrarily large weights in  $\Psi$ , and strongly interacting (large  $U$ ) systems can be treated.

The corresponding self-energies of the various approximations are shown in Fig. 5 (we plot only the imaginary part,  $\text{Im}\Sigma(i\omega_n)$ ). Again, good qualitative agreement between all the CI methods and ED is observed for all values of  $U/t$ . Indeed, for  $U/t = 4, 6, 20$ , even the simplest CI approximation (CISD) yields an essentially indistinguishable self-energy from ED. Only at  $U/t = 8$  (Fig. 5c) do we see appreciable differences. Here we need to use CAS(2,2)CISDT to achieve less than 1% error in the self-energy. Of course, CAS(2,2)CISDT is also the most accurate approximation to ED as measured by the size of the excitation space.

As discussed in section II A, the accuracy of the CI expansions can be improved by working in the natural orbital basis. Examining the ED calculations at half-filling we find that across the range of different  $U/t$  only 4 natural orbitals have occupancies appreciably different from 0 and 2. Consequently, we choose these 4 active orbitals for an active space calculation in the natural orbital basis. In Fig. 6, we show the spectral functions at half-filling using the CAS(4,4) approximation, in the natural orbital basis of the ED calculation. Note that the CAS(4,4) wavefunction involves *only 16 determinants* but the spectral functions are still remarkably similar to the ED spectral functions. In fact, they are of similar quality to the CAS(2,2)CISD spectral functions (also in the natural orbital basis). This demonstrates the compactness of the natural orbital description.

### 2. away from particle-hole symmetry

We next consider the 1D Hubbard model away from half-filling. The corresponding imaginary parts of the self-energies, for  $U/t = 6$  and dopings of 5% – 30%, are shown in Fig. 7 for CISD, CISDT, and CAS(2,2)CISD. To better illustrate the differences between the methods, here we plot the percentage error in the imaginary part of the self-energies, relative to ED. While all the CI approximations yield qualitatively reasonable self-energies, we see that when we include triple excitations, the errors become significantly less than 1%. This is consistent with our expectation that away from half filling, the wave function of this model becomes more single-determinantal and therefore it is more advantageous to base the description on a single reference determinant (in this case the HF determinant) than to include multiple determinant reference wave functions as

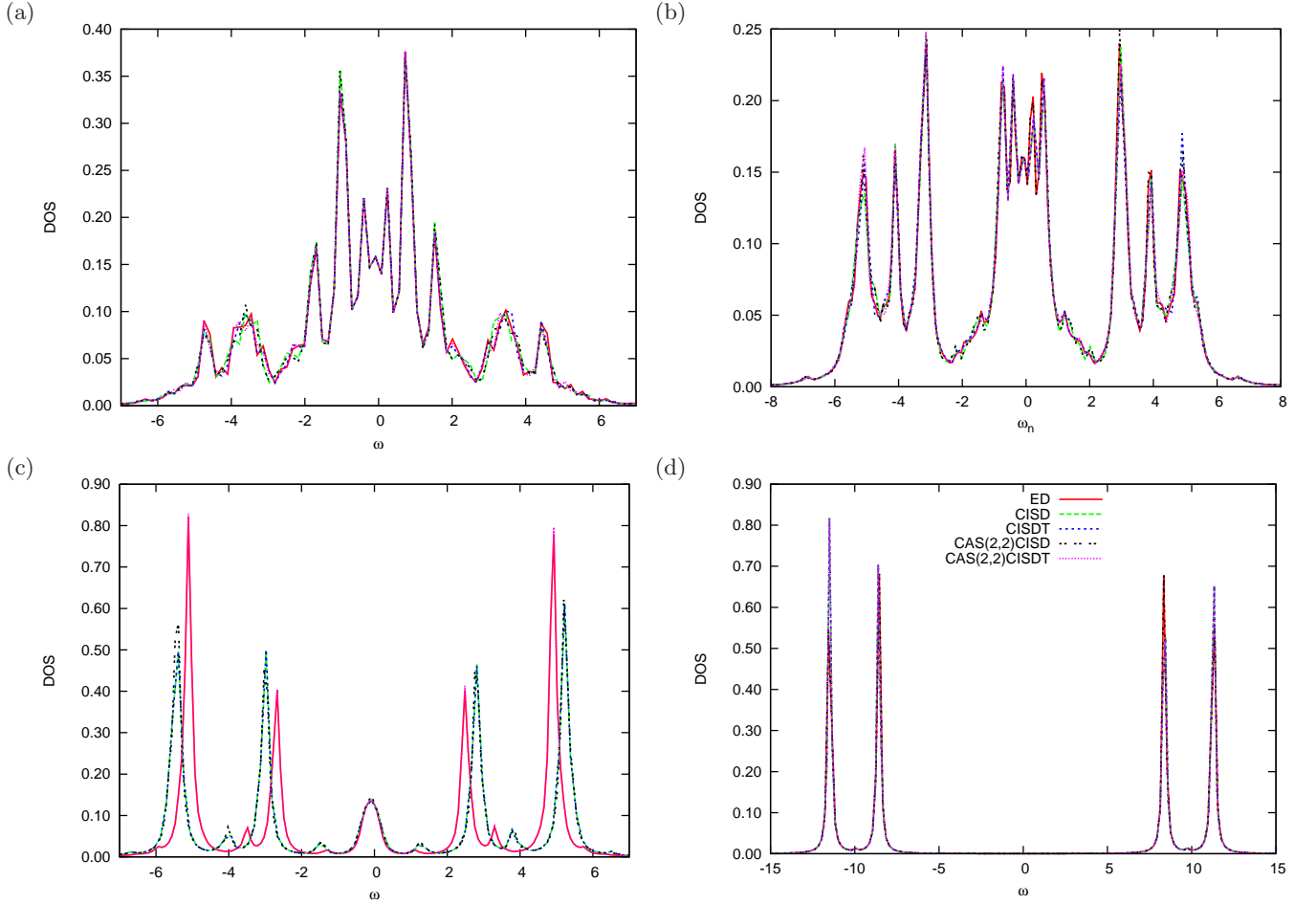


FIG. 4. Single site DMFT approximation to the 1D Hubbard model at half-filling, using 11 bath orbitals: Spectral function (DOS)  $A(\omega) = -\frac{1}{\pi}\text{Im}G(\omega)$ . Solid lines (red online): ED. Light dashed line (green online): CISD. Dark dashed line (blue online): CISDT. Double dotted line (black online): CAS(2,2)CISD. Dotted line (magenta online): CAS(2,2)CISDT. (a)  $U/t = 4$ , (b)  $U/t = 6$ , (c)  $U/t = 8$ , (d)  $U/t = 20$ . Note that panel (a) is similar (but not completely identical) to Fig. 3, where all methods used the converged ED parameters of Tab. I for solving the impurity Hamiltonian.

in CAS(2,2)CISD.

### C. 4-site cellular DMFT approximation to the 2D Hubbard model

We now turn to cluster dynamical mean field theory, and in particular the  $2 \times 2$  cellular DMFT approximation<sup>10,25</sup> of the 2D Hubbard model. We begin with a 12 orbital quantum impurity model using 8 bath orbitals, corresponding to 2 bath orbitals per impurity site, a model that has been extensively studied in previous ED calculations.<sup>27–30</sup> In common with these studies, we use the 4-fold symmetry of the  $2 \times 2$  cluster and calculate the Green's function and self-energies in the symmetry adapted basis of the cluster. In this basis, the Green's functions and self-energies become diagonal. Labeling the sites of the  $2 \times 2$  cluster as  $1 \equiv (0, 0)$ ,  $2 \equiv (1, 0)$ ,  $3 \equiv (0, 1)$ ,  $4 \equiv (1, 1)$ , the symmetry orbitals

$\Gamma$ ,  $M$ ,  $X$  (doubly degenerate) are given by

$$\psi_{\Gamma} = \frac{1}{2}(\phi_1 + \phi_2 + \phi_3 + \phi_4) \quad (9)$$

$$\phi_M = \frac{1}{2}(\phi_1 - \phi_2 - \phi_3 + \phi_4) \quad (10)$$

$$\phi_X = \frac{1}{2}(\phi_1 + \phi_2 - \phi_3 - \phi_4) \quad (11)$$

$$\phi_{X'} = \frac{1}{2}(\phi_1 - \phi_2 + \phi_3 - \phi_4) \quad (12)$$

The symmetry orbitals  $\phi_X$  and  $\phi_{X'}$  form a degenerate pair. For a detailed description of this model see e.g. Refs. 29 and 30.

We carried out CISD, CISDT, CAS(2,2)CISD, CAS(2,2)CISDT, CAS(2,2)CISDTQ, and ED calculations of the spectral functions and self-energies at half-filling. The CI calculations were carried out in the natural orbital basis of a CAS(2,2)CISD calculation in the Hartree-Fock basis.

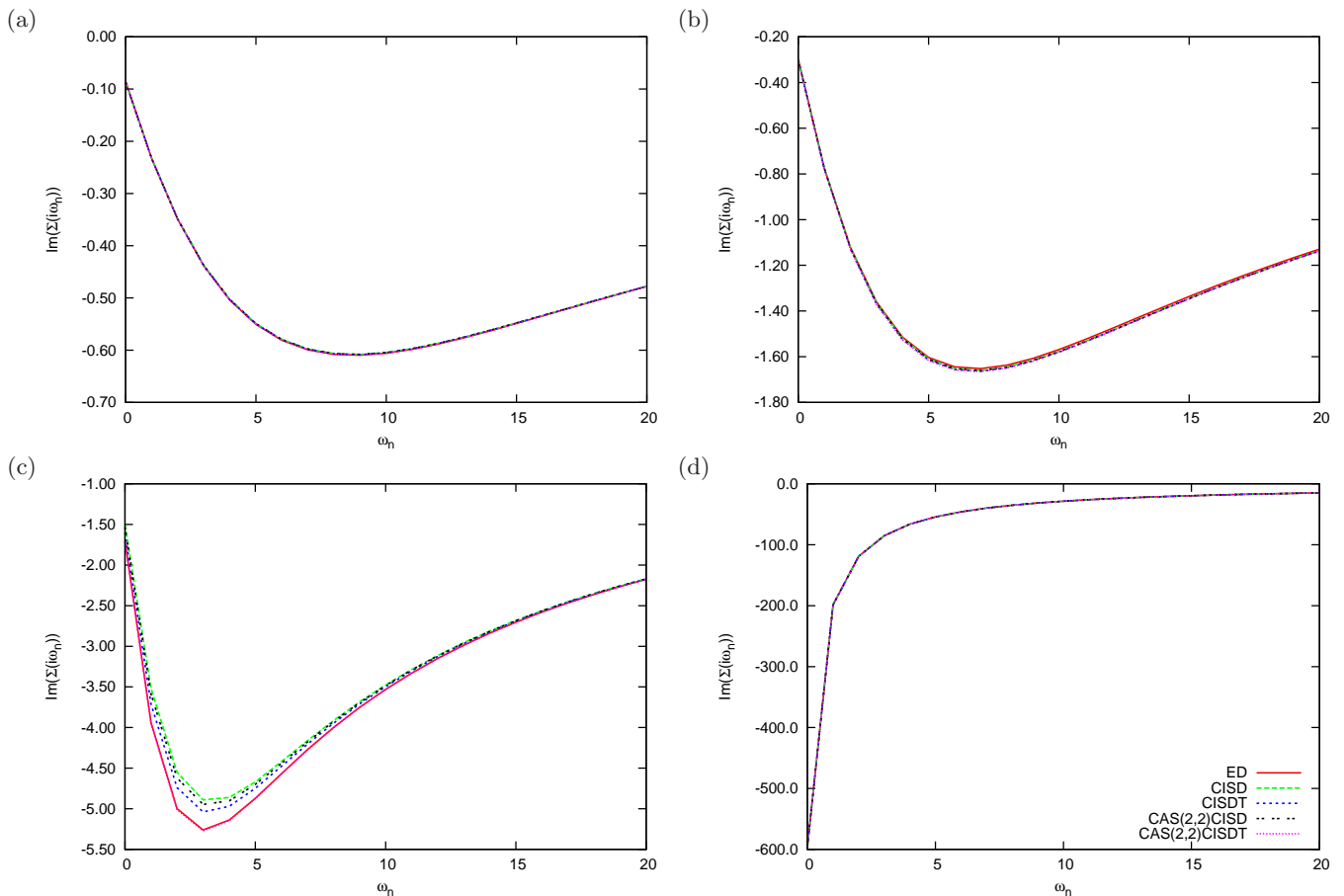


FIG. 5. single site DMFT approximation to the 1D Hubbard model at half-filling, using 11 bath orbitals: Imaginary part of self-energy  $\text{Im}\Sigma(i\omega_n)$ , with Matsubara frequencies  $\omega_n = (2n + 1)\pi/\beta$  for  $\beta t = 20$ . Methods as in Fig. 4. (a)  $U = 4$ , (b)  $U = 6$ , (c)  $U = 8$ , (d)  $U = 20$ .

The local spectral functions  $-\frac{1}{4\pi}\text{TrIm}G(\omega)$  are shown in Fig. 8. The imaginary parts of the  $X$  self-energy,  $\text{Im}\Sigma_X(\omega)$ , corresponding to Eq. 11, are shown in Fig. 9. Similar to the 1D case, we find good agreement between all the CI methods and ED for all studied values of  $U/t$ , although there are some visible differences between CAS(2,2)CISD and ED. Once triple and higher excitations are included, however, the spectral functions become indistinguishable to the eye. The same conclusion can be drawn from analyzing the self-energies. While CAS(2,2)CISD is qualitatively similar to ED, the self-energy for  $U/t = 4$  is shifted from the ED self-energy, with the errors largest at small frequencies. Once triples are included, the agreement becomes much better, and with quadruples the self-energy is indistinguishable from that of ED. If we consider CAS(2,2)CISDT as yielding quantitative agreement, then this is achieved using 49644 determinants in the CI expansion, or only about 6% of the ED determinantal space.

In this model, we find that the most difficult values of  $U/t$  to achieve agreement between the CI methods and ED are for  $U/t = 4$  and  $U/t = 5$ . Here, the form of the

self-energy is that of a correlated Fermi liquid with a large effective mass. This behavior appears in the vicinity of the first-order cluster DMFT metal-insulator transition which, in CT-QMC simulations, is near  $U/t = 5.4$ .<sup>33,36</sup> (Note that in this pseudogap region, ED calculations can actually converge to two different correlated metallic solutions, depending on the initial guess for the bath parametrization, a feature which is repeated in the CI calculations. We have chosen to present the more insulating solution in Fig. 9).

We now briefly turn to some calculations on this model which cannot be performed using ED. An essential weakness of ED (and CI) solvers in the DMFT context is the need to parametrize the bath using a finite number of bath orbitals. If the number of bath orbitals is too small, the resolution of the spectral function and other quantities is very low, and furthermore, artifacts can appear in the ED calculations due to a large fitting error at low frequencies.<sup>30,37,38</sup> CI approximations, however, allow us to treat larger numbers of orbitals, and thus potentially alleviate the bath parametrization problem by allowing us to use a sufficient number of bath orbitals. We now



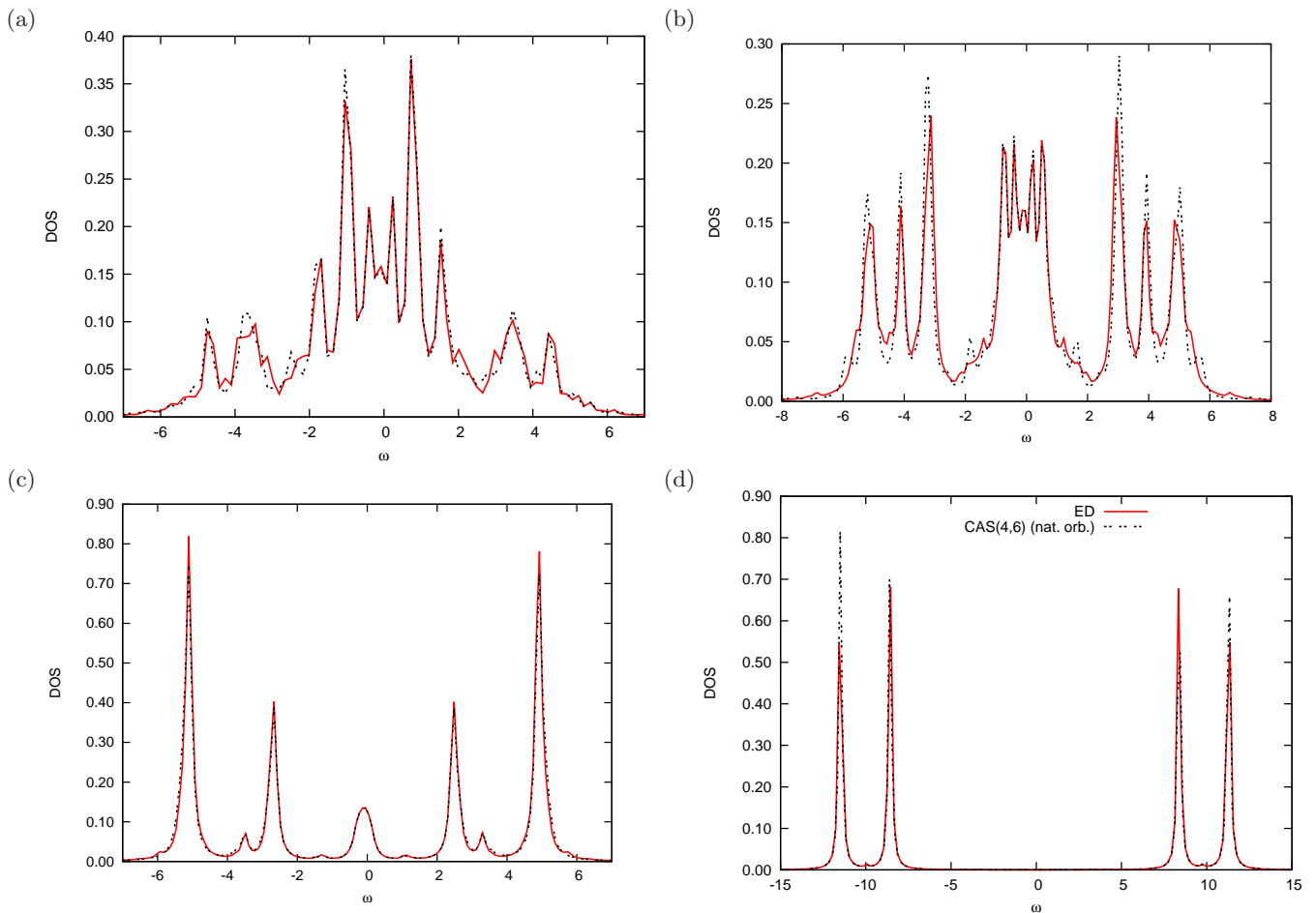


FIG. 6. Single site DMFT approximation to the 1D Hubbard model at half filling, using 11 bath orbitals: Spectral function (DOS)  $A(\omega) = -\frac{1}{\pi}\text{Im}G(\omega)$  Comparison between CAS(4,4) in the natural orbital basis (black dots) and ED (solid line). (a)  $U/t = 4$ , (b)  $U/t = 6$ , (c)  $U/t = 8$ , (d)  $U/t = 20$ .

demonstrate this for the  $2 \times 2$  cluster. In Fig. 10 we plot the self-energies for  $U/t = 8$  from CAS(2,2)CISD calculations (using the CAS(2,2)CISD natural orbital basis) and for 8, 16, and 24 bath orbitals. For 12 bath orbitals we used CAS(4,4)CISD rather than CAS(2,2)CISD for technical reasons due to the degeneracy of the reference wave function. The largest calculation with 24 bath orbitals (or a total of 28 orbitals in the impurity model) is roughly twice the size of what can be treated with ED. Our studies confirm that convergence in this model is achieved fairly rapidly, but that there are nonetheless quantitative differences between the standard 8 bath orbital parametrization and larger bath representations, particularly for small frequencies. The 16 bath orbital and 24 bath orbital parametrizations are indistinguishable, indicating that full convergence has been reached. We have also carried out calculations for other values of  $U/t$ , where we observe similar convergence behavior. The convergence of the bath parametrization appears slower for  $U/t = 5$  and  $U/t = 6$ , which may once again be related to the proximity to a metal-insulator transition.

## V. CONCLUSIONS

In the current work we have described how configuration interaction (CI) approximations to exact diagonalization (ED) can be used as solvers for quantum impurity models, such as those encountered in dynamical mean-field theory (DMFT). CI solvers form a controlled hierarchy of polynomial cost approximations that retain the main advantages of ED, such as the ability to treat general interactions and obtain real spectral information. As we have demonstrated in this work, the convergence of the CI hierarchy is sufficiently rapid that in many cases, they almost exactly approximate the ED results, at a small fraction of the cost. This is true even in “difficult”, “strongly correlated” regimes, such as the pseudogap regime of the  $2 \times 2$  cluster DMFT of the Hubbard model. In addition, this great increase in computational efficiency potentially allows us to treat considerably larger quantum impurity models than have been considered in ED. In this work we used this ability to demonstrate bath convergence for the  $2 \times 2$  cluster DMFT

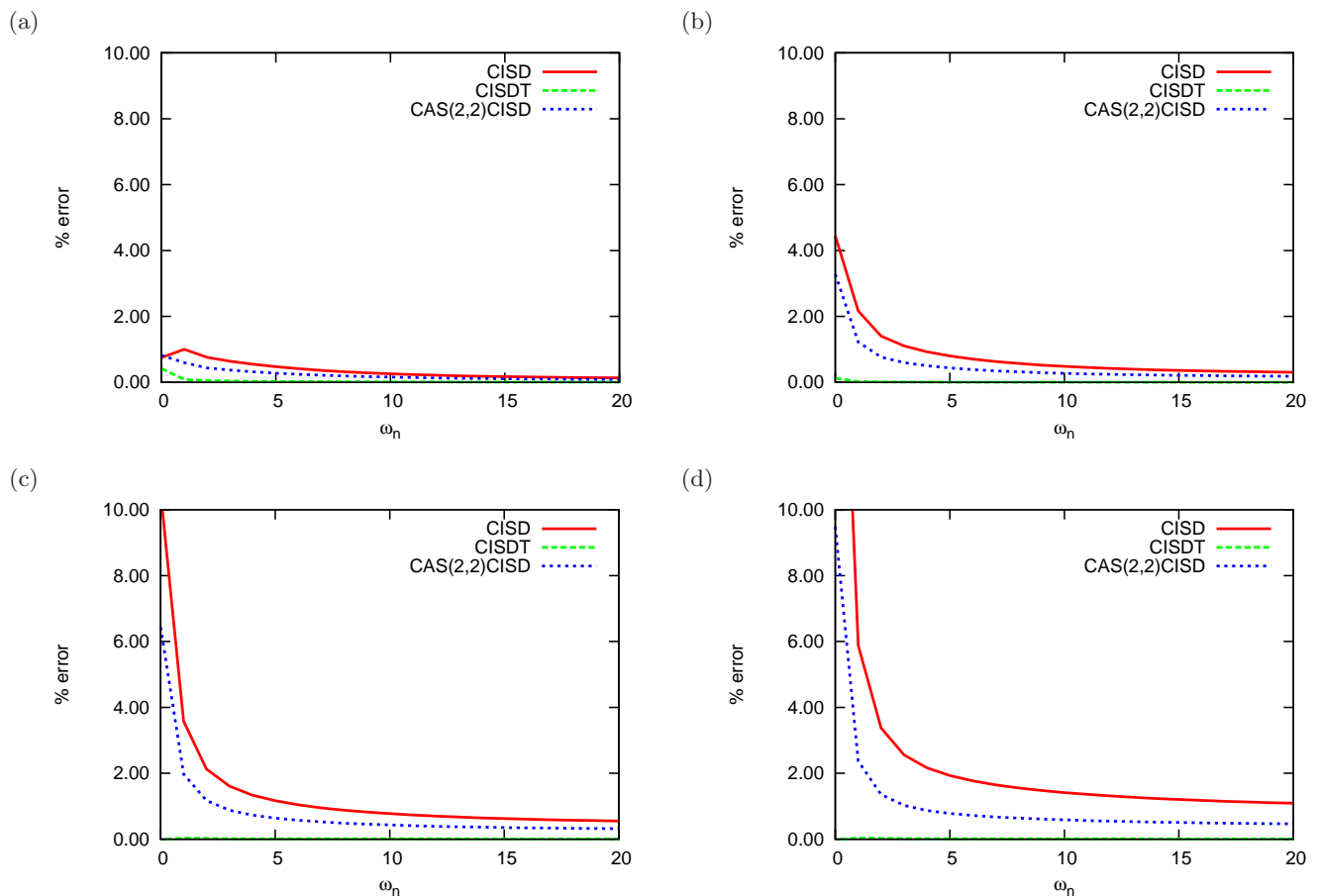


FIG. 7. Single site DMFT approximation to the 1D Hubbard model away from half filling, using 11 bath orbitals: Percent error in the imaginary part of the self-energy  $\text{Im}\Sigma(i\omega_n)$  (relative to ED) for CISD (solid lines, red online), CISDT (dashed lines, green online), and CAS(2,2)CISD (dotted lines). (a) 5% doping, (b) 10% doping, (c) 15% doping, (d) 30% doping.  $\omega_n = (2n + 1)\pi/\beta$ ,  $\beta t = 20$ .

of the Hubbard model in a calculation with 28 orbitals, for a case where previously only 12 orbitals (Lanczos) were accessible.

Here we have focused on well studied DMFT problems in order to benchmark the CI approximations. In future work, we plan to apply these CI approximations to study problems where existing solvers have difficulties. Some of these include impurity models with a large number of orbitals and with general interactions and off-diagonal hybridizations, for which CT-QMC methods encounter a severe sign problem. Another interesting direction to explore will be to examine more sophisticated quantum chemistry approximations to ED. For example, for weak interactions, coupled cluster approximations are known to be far superior to configuration interaction approximations for a given computational cost. These and other directions are currently being pursued.

## ACKNOWLEDGMENTS

Dominika Zgid acknowledges helpful discussions with A.J. Millis, D.R. Reichman, A.I. Lichtenstein, L. de Medici, and A. Liebsch. Dominika Zgid and Garnet Kin-Lic Chan acknowledge support from the Department of Energy, Office of Science, through Award DE-FG02-07ER46432. Emanuel Gull was partially supported by NSF-DMR-1006282.

## Appendix A: Three-orbital model with rotationally invariant interactions

As a further application we present here results for a three-orbital model with general, rotationally invariant interactions. Problems of this type have been notoriously difficult to solve, as quantum Monte Carlo impurity solvers for multi-orbital models are either limited to density-density interactions<sup>39,40</sup> or suffer from a severe

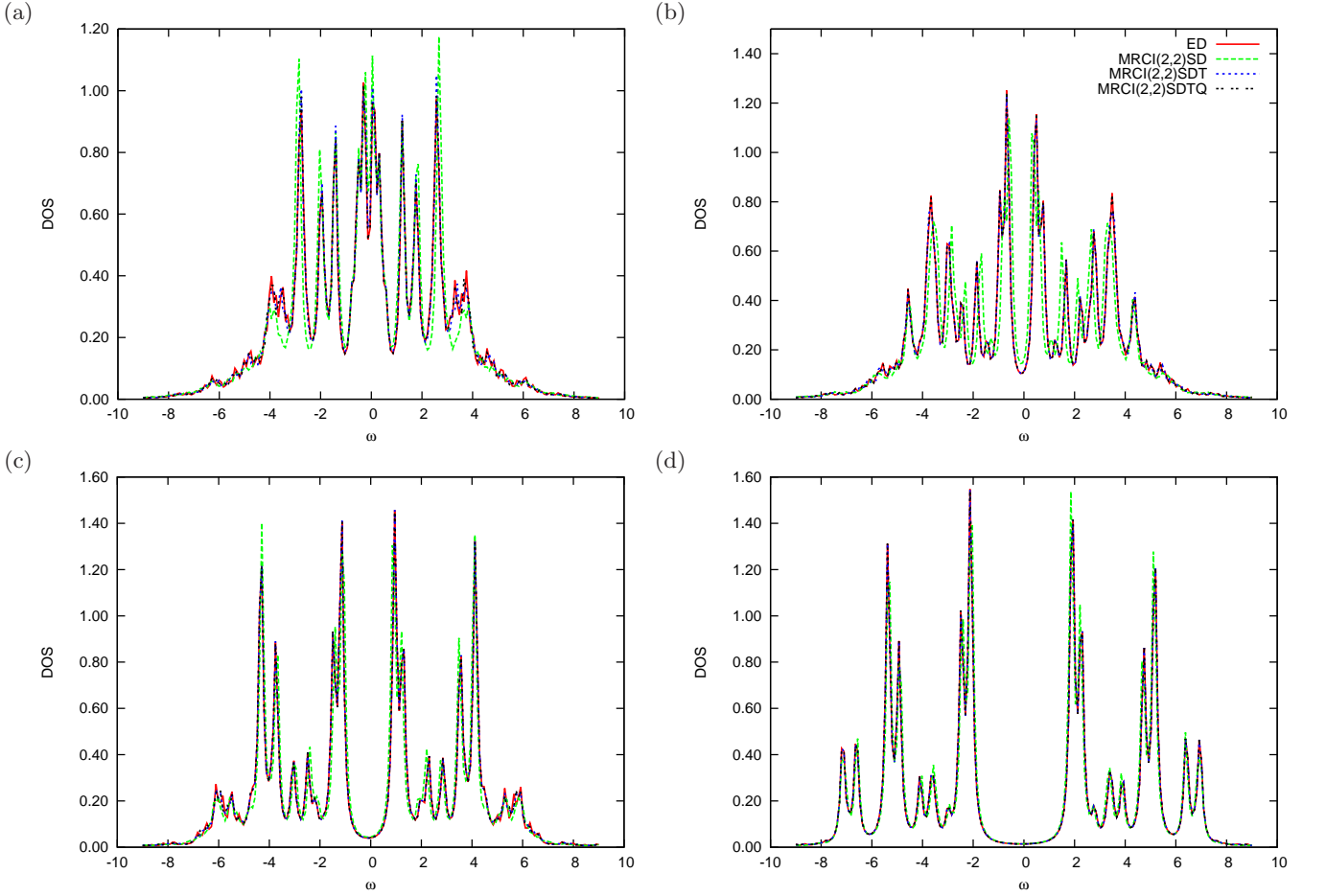


FIG. 8. Cellular dynamical mean field approximation to the  $2D$  Hubbard model at half filling on a  $2 \times 2$  cluster using 8 bath orbitals: Local spectral function (DOS)  $A(\omega) = -\frac{1}{\pi} \text{TrIm}G(\omega)$ . For a description of the methods see text. (a)  $U/t = 4$ , (b)  $U/t = 5$ , (c)  $U/t = 6$ , (d)  $U/t = 8$ .

fermionic sign problem, even at half-filling.<sup>41–43</sup> So far, only the continuous-time hybridization expansion<sup>44,45</sup> and exact diagonalization methods<sup>46</sup> have been able to access this regime, but the exponential scaling of the local impurity Hilbert space size makes five- and seven-orbital systems inaccessible without severe truncations or fitting errors.<sup>11</sup>

The three orbital model with the Slater-Kanamori<sup>34,35</sup> form of the Hamiltonian,

$$\begin{aligned}
 H_{\text{loc}} = H_{\text{SK}} \equiv & U \sum_a n_{a\uparrow} n_{a\downarrow} + (U - 2J) \sum_{a \neq b} n_{a\uparrow} n_{b\downarrow} \\
 & + (U - 3J) \sum_{a > b, \sigma} n_{a\sigma} n_{b\sigma} \\
 & - J \sum_{a \neq b} \left( d_{a\uparrow}^\dagger d_{a\downarrow}^\dagger d_{b\uparrow} d_{b\downarrow} + d_{a\uparrow}^\dagger d_{b\downarrow}^\dagger d_{b\uparrow} d_{a\downarrow} \right), \quad (\text{A1})
 \end{aligned}$$

on a Bethe lattice is a toy model that has been well studied with these methods<sup>46–49</sup> and shows interesting spin-freezing behavior as a function of the Hund's coupling  $J$ . We show in Fig. 11 the imaginary part of the self-energy at half filling (in the Mott insulating phase), for  $U/t = 12$  and  $J/t = 1$ . As in the case of the single- and four-orbital models, convergence to the ED solution for a fixed number of bath sites and convergence as a function of the number bath sites is observed, and we find no additional complications caused by the more general interaction structure.

<sup>1</sup> P. W. Anderson, Phys. Rev. **124**, 41 (1961).

<sup>2</sup> R. Hanson, L. P. Kouwenhoven, J. R. Petta,

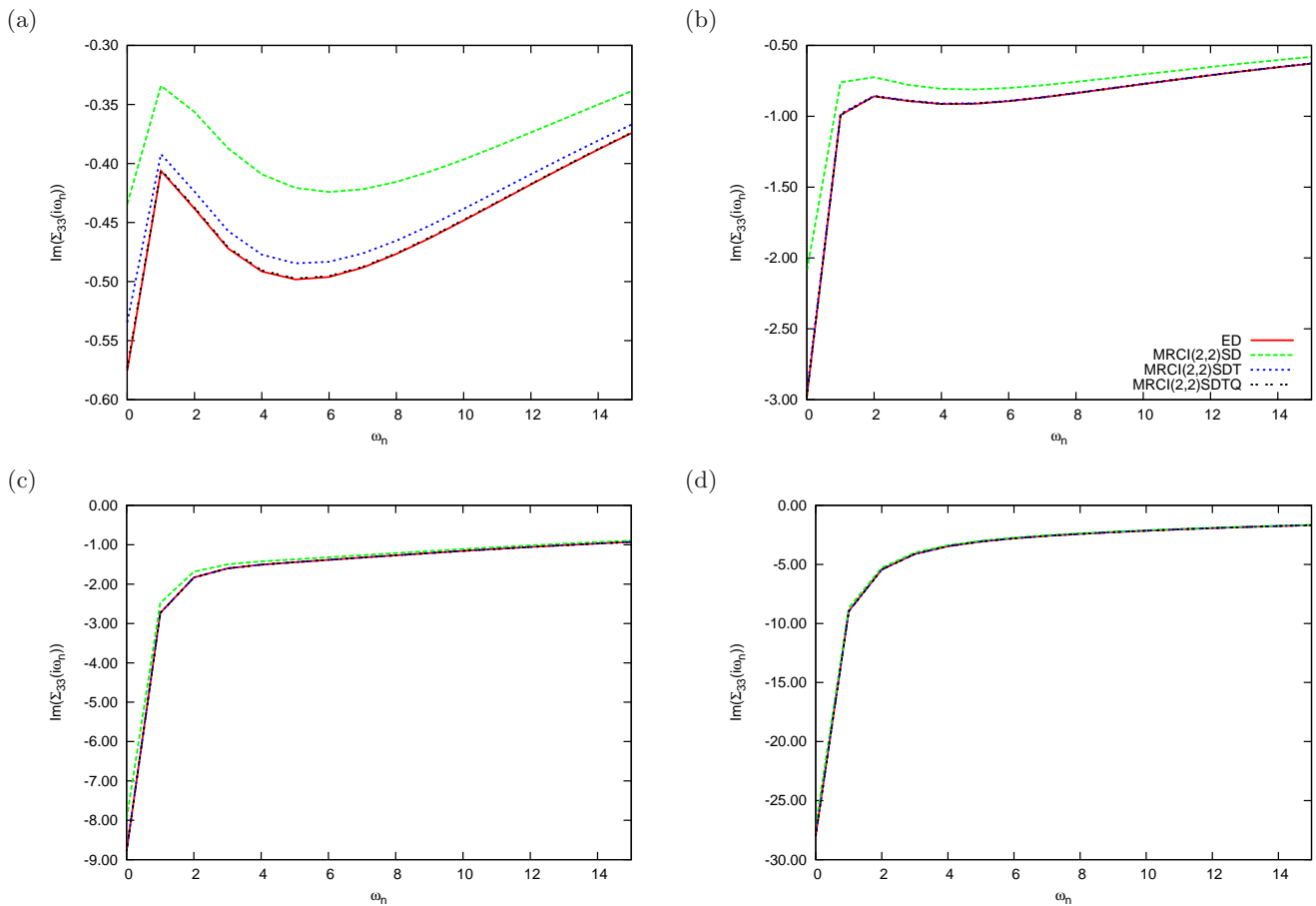


FIG. 9. Cellular dynamical mean field approximation to the  $2D$  Hubbard model at half filling on a  $2 \times 2$  cluster using 8 bath orbitals: Imaginary part of the self-energy  $\text{Im}\Sigma_{33}(i\omega_n)$ . For a description of the methods see text. (a)  $U/t = 4$ , (b)  $U/t = 5$ , (c)  $U/t = 6$ , (d)  $U/t = 8$ .  $\omega_n = (2n + 1)\pi/\beta$ ,  $\beta t = 12.5$ .

- S. Tarucha, and L. M. K. Vandersypen, *Reviews of Modern Physics* **79**, 1217 (2007).
- <sup>3</sup> R. Brako and D. M. Newns, *Journal of Physics C: Solid State Physics* **14**, 3065 (1981).
- <sup>4</sup> K. G. Wilson, *Rev. Mod. Phys.* **47**, 773 (1975).
- <sup>5</sup> I. Affleck, "Quantum impurity problems in condensed matter physics," *International Conference on Strongly Correlated Electron Systems - SCES 2005* (2008), arXiv:0809.3474.
- <sup>6</sup> W. Metzner and D. Vollhardt, *Phys. Rev. Lett.* **62**, 324 (1989).
- <sup>7</sup> A. Georges and W. Krauth, *Phys. Rev. Lett.* **69**, 1240 (1992).
- <sup>8</sup> A. Georges, G. Kotliar, W. Krauth, and M. J. Rozenberg, *Rev. Mod. Phys.* **68**, 13 (1996).
- <sup>9</sup> G. Kotliar, S. Y. Savrasov, K. Haule, *et al.*, *Rev. Mod. Phys.* **78**, 865 (2006).
- <sup>10</sup> T. Maier, M. Jarrell, T. Pruschke, and M. H. Hettler, *Rev. Mod. Phys.* **77**, 1027 (2005).
- <sup>11</sup> E. Gull, A. J. Millis, A. I. Lichtenstein, A. N. Rubtsov, M. Troyer, and P. Werner, *Rev. Mod. Phys.* **83**, 349 (2011).
- <sup>12</sup> R. Bulla, A. C. Hewson, and T. Pruschke, *Journal of Physics: Condensed Matter* **10**, 8365 (1998).
- <sup>13</sup> R. Bulla, T. A. Costi, and T. Pruschke, *Rev. Mod. Phys.* **80**, 395 (2008).
- <sup>14</sup> D. J. García, K. Hallberg, and M. J. Rozenberg, *Phys. Rev. Lett.* **93**, 246403 (2004).
- <sup>15</sup> S. Nishimoto, F. Gebhard, and E. Jeckelmann, *Physica B: Condensed Matter* **378-380**, 283 (2006), proceedings of the International Conference on Strongly Correlated Electron Systems - SCES 2005.
- <sup>16</sup> M. Caffarel and W. Krauth, *Phys. Rev. Lett.* **72**, 1545 (1994).
- <sup>17</sup> K. Held, I. A. Nekrasov, G. Keller, V. Eyert, N. Bluemer, A. K. McMahan, R. T. Scalettar, T. Pruschke, V. I. Anisimov, and D. Vollhardt, *Phys. Status Solidi* **243**, 2599 (2006).
- <sup>18</sup> T. Helgaker, P. Jorgensen, and J. Olsen, *Molecular Electronic-Structure Theory* (Wiley, 2000).
- <sup>19</sup> D. Zgid and G. K.-L. Chan, *The Journal of Chemical Physics* **134**, 094115 (2011).
- <sup>20</sup> C. F. Bender and E. R. Davidson, *The Journal of Physical Chemistry* **70**, 2675 (1966), <http://pubs.acs.org/doi/pdf/10.1021/j100880a036>.
- <sup>21</sup> C. D. Sherrill and H. F. Schaefer III, in *The Configuration Interaction Method: Advances in Highly Correlated* *Advances in Quantum Chemistry*, Vol. 34, edited by P.-O. Lwidi, J. R. Sabin, M. C. Zerner, and E. Brndas (Academic Press, 1999) pp. 143 – 269.

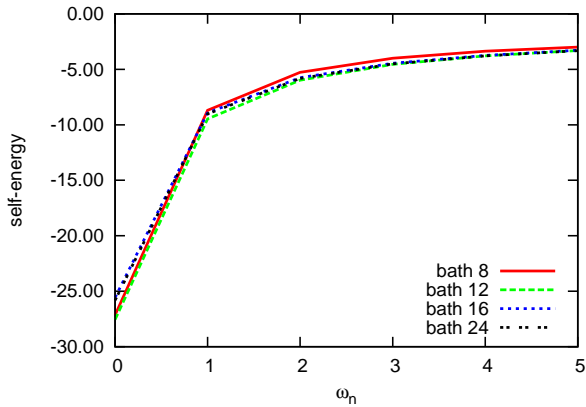


FIG. 10. Cellular dynamical mean field approximation to the 2D Hubbard model at half filling on a  $2 \times 2$  cluster for a range of bath sites: Imaginary part of the self-energy  $\text{Im}\Sigma_{33}(i\omega_n)$ . The CI method used was CAS(2,2)CISD in the natural orbital basis of CAS(2,2)CISD.

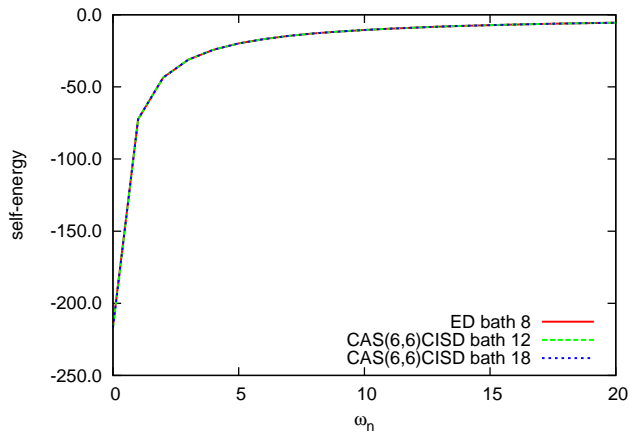


FIG. 11. Dynamical mean field approximation to the 3-orbital Hubbard model at half filling: Imaginary part of the self-energy  $\text{Im}\Sigma(i\omega_n)$  for ED (solid lines, red online) with 12 bath sites, CAS(6,6)CISD with 15 bath sites, and CAS(6,6)CISD with 21 bath sites. Differences are on the order of 0.5%.

<sup>22</sup> “Dalton, a molecular electronic structure program, release 2.0,” <http://daltonprogram.org/> (2005).

<sup>23</sup> E. R. Davidson, *Journal of Computational Physics* **17**, 87 (1975).

<sup>24</sup> C. Lanczos, *Journal of Research of the National Bureau of*

*Standards* **45** (1950).

<sup>25</sup> G. Kotliar, S. Y. Savrasov, G. Pálsson, and G. Biroli, *Phys. Rev. Lett.* **87**, 186401 (2001).

<sup>26</sup> A. I. Lichtenstein and M. I. Katsnelson, *Phys. Rev. B* **62**, R9283 (2000).

<sup>27</sup> M. Civelli, M. Capone, S. S. Kancharla, O. Parcollet, and G. Kotliar, *Physical Review Letters* **95**, 106402 (2005).

<sup>28</sup> S. S. Kancharla, B. Kyung, D. Sénéchal, M. Civelli, M. Capone, G. Kotliar, and A.-M. S. Tremblay, *Phys. Rev. B* **77**, 184516 (2008).

<sup>29</sup> A. Liebsch, H. Ishida, and J. Merino, *Phys. Rev. B* **78**, 165123 (2008).

<sup>30</sup> A. Liebsch and N.-H. Tong, *Phys. Rev. B* **80**, 165126 (2009).

<sup>31</sup> K. Haule, *Physical Review B (Condensed Matter and Materials Physics)*

<sup>32</sup> E. Gull, P. Werner, X. Wang, M. Troyer, and A. J. Millis, *EPL (Europhysics Letters)* **84**, 37009 (6pp) (2008).

<sup>33</sup> H. Park, K. Haule, and G. Kotliar, *Physical Review Letters* **101**, 186403 (2008).

<sup>34</sup> T. Mizokawa and A. Fujimori, *Phys. Rev. B* **51**, 12880 (1995).

<sup>35</sup> M. Imada, A. Fujimori, and Y. Tokura, *Rev. Mod. Phys.* **70**, 1039 (1998).

<sup>36</sup> G. Sordi, K. Haule, and A.-M. S. Tremblay, *Phys. Rev. Lett.* **104**, 226402 (2010).

<sup>37</sup> E. Koch, G. Sangiovanni, and O. Gunnarsson, *Phys. Rev. B* **78**, 115102 (2008).

<sup>38</sup> D. Sénéchal, *Phys. Rev. B* **81**, 235125 (2010).

<sup>39</sup> J. E. Hirsch and R. M. Fye, *Phys. Rev. Lett.* **56**, 2521 (1986).

<sup>40</sup> E. Gull, P. Werner, O. Parcollet, and M. Troyer, *EPL (Europhysics Letters)* **82**, 57003 (2008).

<sup>41</sup> S. Sakai, R. Arita, and H. Aoki, *Phys. Rev. B* **70**, 172504 (2004).

<sup>42</sup> A. N. Rubtsov, V. V. Savkin, and A. I. Lichtenstein, *Phys. Rev. B* **72**, 035122 (2005).

<sup>43</sup> S. Sakai, R. Arita, K. Held, and H. Aoki, *Physical Review B (Condensed Matter and Materials Physics)* **74**, 155107 (2006).

<sup>44</sup> P. Werner, A. Comanac, L. de’ Medici, *et al.*, *Phys. Rev. Lett.* **97**, 076405 (2006).

<sup>45</sup> P. Werner and A. J. Millis, *Phys. Rev. B* **74**, 155107 (2006).

<sup>46</sup> A. Liebsch and H. Ishida, *Journal of Physics: Condensed Matter* **24**, 053201 (2012).

<sup>47</sup> P. Werner, E. Gull, M. Troyer, and A. J. Millis, *Physical Review Letters* **101**, 166405 (2008).

<sup>48</sup> P. Werner, E. Gull, and A. J. Millis, *Phys. Rev. B* **79**, 115119 (2009).

<sup>49</sup> L. de’ Medici, J. Mravlje, and A. Georges, *Phys. Rev. Lett.* **107**, 256401 (2011).